Proceedings, Bicycle and Motorcycle Dynamics 2019
Symposium on the Dynamics and Control of Single Track Vehicles,
9 – 11 September 2019, University of Padova, Italy

Evaluation of a Motorcycle Simulator

B.E. Westerhof[*], E.J.H. de Vries[#], R Happee[†], A.L.Schwab[†]

[*] Engibex N.V.
Louizalaan 120, 1050 Brussel, Belgium
e-mail: bernhard.westerhof@gmail.com

[#] Cruden B.V.
Pedro de Medinalaan 25,1086 XP Amsterdam,
the Netherlands
e-mail: e.devries@cruden.com

[†] Faculty 3Me
Delft University of Technology
Mekelweg 2, NL-2628 CD Delft, The Netherlands
e-mail: r.happee@tudelft.nl,a.l.schwab@tudelft.nl

ABSTRACT

The use of motorcycle simulators enables manufacturers to develop new motorcycle technologies taking into account rider behaviour. Unfortunately, few motorcycle simulators are used in the development of new motorcycles and motorcycle safety systems. Furthermore, validation of the available motorcycle simulators is lacking and little design knowledge is available.

This paper presents and evaluates a new motorcycle simulator and shows that it can be used in motorcycle research. The simulator features six degrees of freedom motion, upper body tracking, and stereo vision with head mounted display. The evaluation consists of three parts.

First, a new motorcycle dynamics model based on literature [1] is developed in Simulink and parameterized to represent a Honda CB750 [2]. The motorcycle dynamics model shows realistic ‘countersteering’ or non-minimum phase behavior. The eigenvalues of capsize and weave motion are qualitatively similar to those in the established literature [2].

Second, the simulator actuator dynamics are evaluated and adjusted. The motorcycle simulator uses a Stewart motion platform and handlebar control loader to provide motion cues and force feedback. It is shown that the adjusted Stewart platform and handlebar control loader have ample bandwidth and sufficiently small phase delays to accurately simulate the motorcycle dynamics.

In the third and final part, a human research approach is used to further evaluate the motorcycle simulator. In a speed perception experiment participants were asked to ride three different speeds on an infinite highway. Participants underestimated their riding speed, where speed perception at higher speeds was relatively more accurate. Both results are in agreement with published speed perception experiments in cars. A curve driving experiment was performed to evaluate steering performance and perceived simulator fidelity and workload, exploring effects of simulator motion and rider body tracking. The steering experiment showed good performance, with positive results for fidelity and modest workloads while motion sickness occurred in only a few participants. Platform motion significantly improved the rider’s performance and perception of simulator fidelity. No statistically significant effects of upper body tracking could be established.

Keywords: motorcycle, simulator, fidelity, motion cueing.

1 INTRODUCTION

Motorcycles are used worldwide for a wide variety of purposes such as commuting, racing and leisure. One of the biggest advantages of motorcycles with small displacement combustion engines is that they are very fuel efficient, making them extremely popular in developing countries. But also a motorcycle's performance for a reasonable cost and the thrill of riding a motorcycle are appealing to their owners. Unfortunately, motorcyclists were 35 times more likely to die in a crash compared to car drivers, per mile travelled, in the U.S. in 2007 [4]. Therefore, research in the field of motorcycle safety is necessary for the development of safer motorcycles to decrease the number of deaths.

Motorcycles have not received the same attention in the development of safety mechanisms as passenger cars and trucks. This could partially be explained by a lack of motive for motorcycle manufacturers, as fast motorcycles sell better than safe motorcycles. But next to that, the means for the development of safety mechanism for motorcycles have also been less available. An example is that motorcycle simulators are rare and even more rarely used in the development of motorcycle safety systems and design. This is interesting to see, as simulators are widely used throughout the aviation and car industry for development of new technologies and training pilots and drivers. After all, simulators offer great flexibility and control over the independent variables, which is not possible in the real world, let alone for safety reasons.

Still one of the first motorcycle simulators was developed by Honda as the Japanese government required simulator training as a part of obtaining the motorcycle license [5]. Other noteworthy motorcycle simulators have been developed over the years by YNL Tokyo, MORIS, Stedmon et al., SIMACOM and SafeBike [5][6][7][8][9]. In 2007 Cruden joined this list by developing its first motorcycle simulator prototype. Recent technical advances like HMD vision and infrared upper-body tracking inspired the development of a new motorcycle driving simulator by Cruden which is the subject of this study.

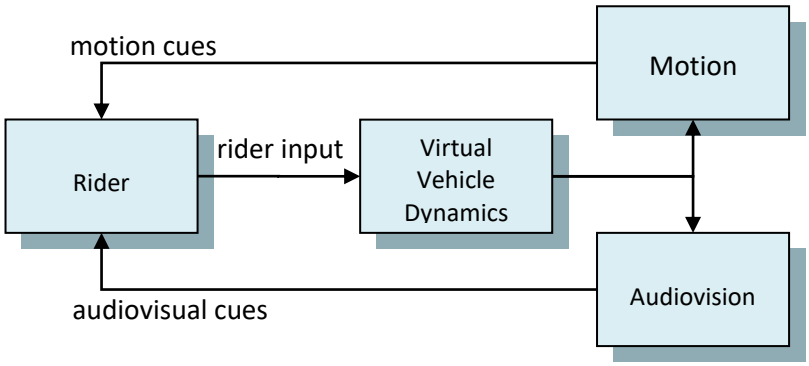

Figure 1. Basic block scheme of a vehicle simulator. The rider provides a certain input to a measurement device which sends the input to the computer running the vehicle dynamics model. The virtual vehicle dynamics model calculates the states of the model. These states are used for representing motion by a motion platform and simulation of other sensory inputs like vision and sound.

In Figure 1 the basic architecture of a driving simulator is shown. It can be seen that vehicle dynamics plays the central role in the simulation of motion and therefore in motorcycle simulators. Research in motorcycle and bicycle dynamics already has a long history, with one of the first papers written by Whipple in 1899 on the stability of bicycles [10][11]. Sharp already mentioned in 1971 that theoretical studies on car steering behavior helped the car industry develop better vehicles and that he wanted to do the same for motorcycles [2]. Early contributors in the field of motorcycle dynamics include among others Sharp, Koenen and Cossalter [12], [13]. Sharp's contributions helped identify motorcycle instabilities like wobble and weave and paved the way for more complex motorcycle dynamics research. Specifically referring to vehicle dynamics in a simulator, Sharp and Limebeer give a good overview of what is needed to model the most important dynamics properties of a motorcycle by using a multibody dynamics modeling

approach [14]. These dynamics properties include the motorcycle's eigenmodes and input-output behavior. Furthermore, results published by Cossalter showed resemblance between an instrumented motorcycle and the SafeBike motorcycle simulator [15].

Looking at motion, it is suggested that roll and pitch motion are the most important, but a comparative research has not been successfully done yet for motorcycle simulators. Since riding a motorcycle is such a dynamic endeavour, it may very well be that the only way of accurate simulation is by providing motion in all degrees of freedom. If, however, motion cues in only certain directions provide satisfactory results, it could be concluded that cheaper simulator constructions can do the job just as well. Numerous studies on the influence of motion have been done in the aviation industry [17][18] and the car industry [19][20][21]. A general conclusion is that motion cueing is preferred by the users and that motion sickness is reduced, thus improving the subjective quality of the simulator. Yet, the challenge remains to prove an increase in simulator validity and objective performance metrics by using motion.

It is suggested that the most important steering input is the handlebar torque [14]. Hence, all motorcycle simulators measure the torque the rider inputs on the simulator's handlebar. However, another interesting topic is rider body motion. As every motorcyclist knows, moving your body on a motorcycle steers the motorcycle [16]. In a study where a 12-DoF rider model has been developed, rider motion did show to influence the motorcycle's behavior [22]. Two examples where rider motion is accounted for are the Safebike motorcycle simulator, where load cells in the foot-pegs are used to account for rider motion and the DESMORI simulator, where an induced roll torque in the simulator is measured resulting from the rider shifting weight [15],[23]. Assessing how riders actually steer their bike would be a valuable contribution to motorcycle research. Using the upper body tracking sensors available on the Cruden Motorcycle Simulator, this study will explore the benefits of implementing upper-body movement as rider input to the motorcycle simulator.

Since the dynamics of a motorcycle strongly depend on the motorcycle's velocity, it is important to know whether users of a motorcycle simulator are able to estimate their speed correctly. Surely, if the perception of velocity on a motorcycle simulator is completely different from that of a real motorcycle, then the motorcycle's dynamics will also be perceived differently. One problem often encountered is that humans are relatively poor in estimating their velocity. For a car, Recarte and Nunes showed that participants underestimated all speeds [24].

The Cruden motorcycle simulator uses a Head-Mounted Display (HMD) to present the visual information to the rider. Another example of a motorcycle simulator using an HMD is the YNL Tokyo simulator [5]. Kemeny and Panerai claim that visual cues are essential for speed perception: HMD's add properties like motion parallax and stereopsis that are which favourable for perception of speed [19]. Specifically for motorcycle simulators, Will has performed extensive studies in speed perception in motorcycle simulators for different sensory inputs [23]. He used mainly presence as a measure of simulator quality. In his research, he used a real motorcycle for his speed perception experiments, and showed that participants underestimated speed with 13 percent error at 50 km/h. However, participants were able to estimate their speed correctly at 100 km/h.

Despite the technological advances incorporated into the new Cruden motorcycle simulator, first subjective tests showed that the simulator was not as agile as expected, especially at low speeds. A thorough analysis of the simulator software and hardware, specifically of the steering system was a prerequisite in our research. These topics are described in section 2 and 3 respectively. The next research question is related to the perceived handling of the simulator. The dynamics of a motorcycle model and the responsiveness to the rider's input are highly dependent on the driving speed. If the rider is consequently underestimating his speed on the motorcycle he misinterprets the dynamic response that he expects at that speed. Understanding the speed perception of the rider allows us to relate that to future subjective handling assessment. The following

hypotheses for the speed perception research have been derived from the work of Recarte and Nunes and [24]:

- Riders have the best speed perception at 120 km/h, underestimating with 5% error.
- Riders have the worst speed perception at 50 km/h, underestimating with 30% error.
- Riders have medium speed perception at 80 km/h, underestimating at 20% error.

These hypotheses are verified using simulator studies with a group of participants that is described in section 4.1, the results of the experiments are given in section 4.2. The third phase of the work evaluates the motorcycle simulator by investigating the importance of platform motion and upper body tracking. The hypotheses investigated are:

- With motion cueing and body tracking, the rider performs best, reports the lowest effort and sickness and highest presence.
- With either motion or body tracking turned off, performance worsens, higher values for effort and sickness are reported and presence is lower.

The results on this second research question are presented in section 4.3, The conclusions are drawn in section 5 of the paper.

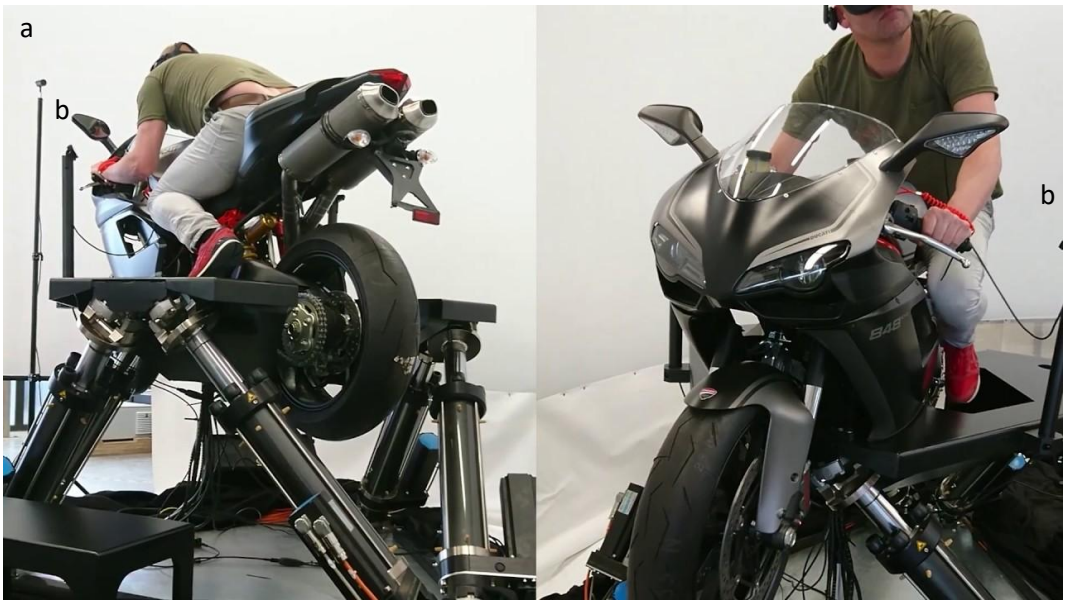

Figure 2. The Cruden motorcycle simulator consisting of a Ducati 848 evo motorcycle mock-up mounted on a Stewart 6-DoF motion platform. Visualization of the virtual scenery by means of head mounted display (HMD).

2 MOTORCYCLE MODEL

A motorcycle model described and validated by Sharp and Alstead in [25] has been adopted. This model contains a parametric description of a Honda CB-750 motorcycle which has been combined with several components models developed at Cruden, including tires, driveline and brake systems. The motorcycle model is developed in Simulink® using the Simscape Multibody™ first generation toolbox (SimMechanics). It consists of six bodies (Figure 3) connected by 7 kinematic joints (Figure 4) with a total of 15 degrees of freedom:

1. Rear frame: six degrees of freedom.
2. Front frame: two degrees of freedom with respect to rear frame, steer angle and frame twist.
3. Front wheel: two degrees of freedom with respect to front frame, one rotational, one prismatic along the front fork rake angle.
4. Rear wheel: two degrees of freedom with respect to rear frame, one rotational, one vertical prismatic.

5. Rider upper body: two planar degrees of freedom with respect to rear frame, longitudinal and lateral.
6. Crankshaft: one rotational degree of freedom with respect to rear frame.

The universal joint between the rear frame and the front frame allows for two rotational degrees of freedom around a rotated x'-z' coordinate system. The z' axis corresponds to the steer axis and the x' axis to the frame flexibility axis. Around the steering axis, a damping of 5 Nms/rad has been added to ensure stability of the model in the driving simulator up to 200km/h. The frame has a finite stiffness of 102 kN/rad derived from Sharp and Alstead [25] with a damping of 2 kNms/rad to keep the simulation numerically stable. The frame compliance is modeled using a native SimMechanics Joint Spring & Damper block across a universal joint.

As mentioned before, the geometry of a motorcycle plays an essential role in its dynamics. Figure 5 gives a schematic representation of the motorcycle's key parameters. Table 1 lists vales of geometric parameters in Figure 5, combined with mass and inertial properties. Subscripts $_f$ and $_r$ correspond to front and rear respectively. Subscript $_r$ corresponds to the rider's body and subscript $_e$ to the engine's crankshaft. Subscript $_w$ indicates wheel properties and subscripts $_{x,y,z}$ correspond to their respective axes.

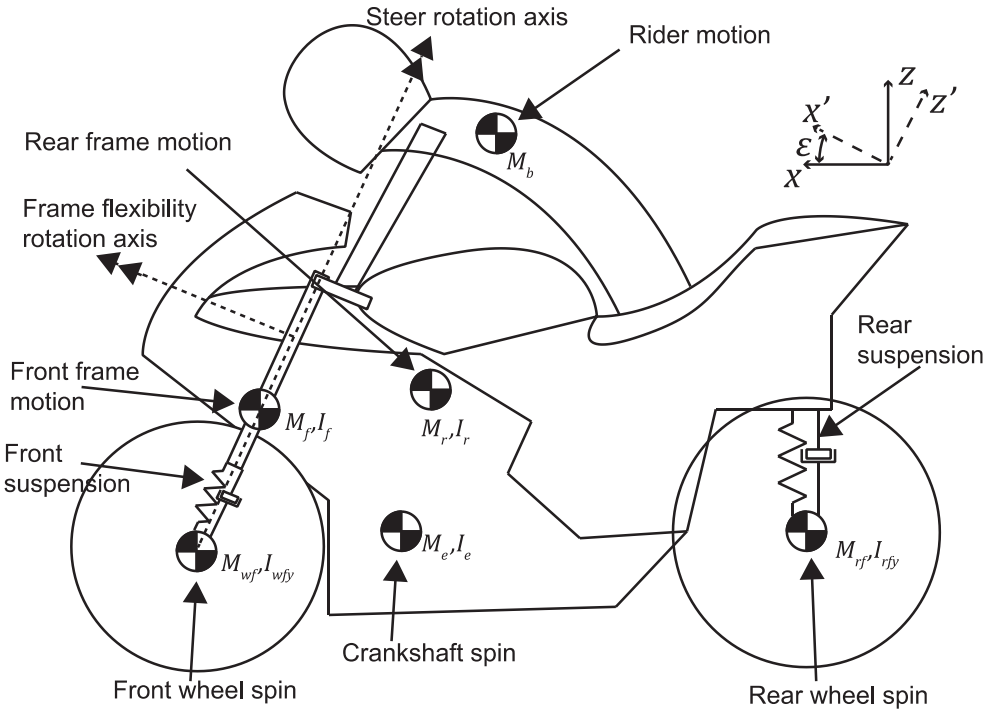

Figure 3. Representation of the motorcycle and rider model indicating the centers of gravity for all bodies accounted for. Based on Sharp and Alstead [25].

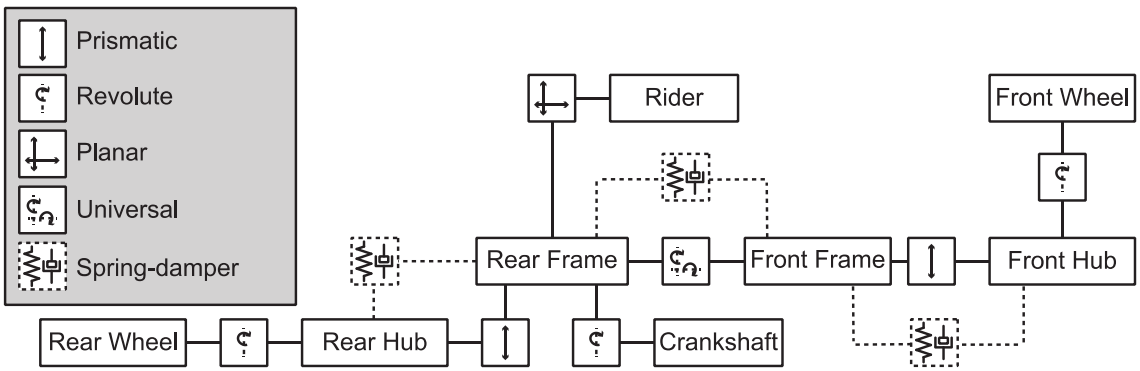

Figure 4. Kinematic joints of the motorcycle model.

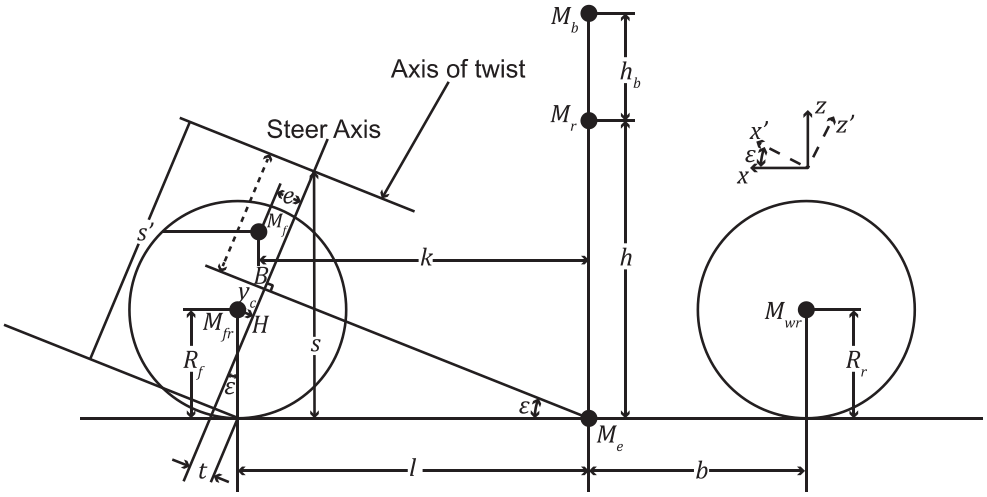

Figure 5. Parameterization of the motorcycle and rider model, based on Sharp and Alstead [25].

Table 1 Geometry and Inertia parameters of the motorcycle model. Based on Sharp and Alstead [25] where parameters marked [1] are adapted to obtain realistic motorcycle pitch and rider upper body dynamics.

Parameter	Value	Unit	Parameter	Value	Unit	Parameter	Value	Unit
b	0.50	m	M_f	25	kg	I_{rx}	32	kgm^2
e	0.05	m	M_r [1]	200	kg	I_{ry} [1]	60	kgm^2
h	0.60	m	M_b [1]	30	kg	I_{rz}	22	kgm^2
j	0.55	m	M_{wf}	10	kg	I_{fx}	3.8	kgm^2
l	0.92	m	M_{wr}	10	kg	I_{fy} [1]	0.0	kgm^2
R_f	0.32	m	M_e [1]	20	kg	I_{fz}	0.3	kgm^2
R_r	0.31	m				I_{wfy}	0.8	kgm^2
t	0.10	m				I_{wry}	1.1	kgm^2
ε	0.47	rad				I_{ex} [1]	0.1	kgm^2
s	0.87	m				I_{ey} [1]	0.1	kgm^2
h_b [1]	0.40	m				I_{ez} [1]	0.1	kgm^2

2.1 Suspension

Both the front and rear suspension kinematics has been modeled as prismatic joints between their respective bodies. The rear suspension is modeled using a Joint Spring & Damper block native to SimMechanics with the following properties: Spring 50 kN/m, Damper 2 kNs/m, Spring Offset -0.02 m.

For the front suspension, Cruden's spring damper system is used, featuring end-stops, bump-stops and non-linear damping characteristics. The stiffness of the front suspension is 20 kN/m, the damper employs a non-linear lookup, and the Spring Offset is 0 m.

Besides the actual suspensions, a virtual roll spring is used to facilitate take off from a standing start with the motorcycle simulator with a stiffness of 100 kNm/rad and damping of 10 kNms/rad at zero velocity, gradually fading out to zero above 3 m/s driving speed.

2.2 Tire modeling

Tire road contact forces are calculated using an extended version of the Magic Formula [26]. Tire deflection is calculated via road height input and tire position. The crown radius is accounted for, and the tire model incorporates additional camber thrust forces, which play an important role in motorcycle tire dynamics [13],[26]. The lateral camber thrust force component, $F_y(\gamma)$ for both the rear and front tire is calculated by:

$$F(\gamma) = -0.65F_z \arcsin(\gamma) \quad (1)$$

where γ is the camber angle, F_z is the tire force in vertical (z) direction and 0.65 is an experimentally determined value. Table 2 lists the most important lumped tire properties that can be extracted from the full MF-tyre 6.1 parameterset at their nominal front and rear wheel load.

Table 2 Lumped motorcycle tire properties.

	Front (F_z = 1184 N)		**Rear** (F_z = 1710 N)	
	longitudinal	*lateral*	*longitudinal*	*lateral*
Stiffness	331.2 kN/m	150.47 kN/m	341.1 kN/m	150.47 kN/m
Slip stiffness	40.84 kN	69.28 kN/rad	64.29 kN	99.41 kN/rad
Relaxation length	61.57 mm	115.1 mm	94.28 mm	165.2 mm

2.3 Driveline

We adopted the SimDriveline model in SimMechanics, consisting of: a) Engine with 3D torque map and control systems, b) Clutch with control systems, c) Gearbox with control systems. Gear ratios are: 4.9524 (primary), 2.4666 (1st) 1.7647 (2rd) 1.4000 (3th) 1.1818 (4th) 1.0435 (5th), 0.9683 (6th). The aerodynamic drag is modeled with a drag coefficient of 0.4 with a frontal area of 0.7 m^2.

2.4 Brakes

Both the front and rear brake are controlled independently. The brake signals are converted to pressure signals, which together with tire velocity, brake temperature, ambient temperature are used to calculate the brake force, brake moment, brake friction and brake temperature.

2.5 Objective validation

A common approach to validating the dynamics of a motorcycle model is to make virtual experiments to identify the eigenmodes of the virtual motorcycle. In this open-loop test the mainframe is excited with a lateral impulse force and the motorcycle model will demonstrate its dynamic response. Motorcycle dynamics is very dependent on driving speed, so it is an important variable to include in the tests: it was varied from 5-50 ms^{-1}. The time response of the roll rate was captured by a representative exponential function with complex coefficients and exponents, where the exponents relate directly to the eigenvalues of the motorcycle model at that speed. Figure 6 presents two example roll rate responses: at the left it can be seen that at 50ms^{-1} the damped oscillating weave is dominant, at the right at 10 ms^{-1} the instable capsize forms the dominant contribution to the bikes response. The eigenvalues that are identified by curve fitting the response are displayed as a root-loci plot in Figure 7. An imaginary part of the eigenvalue indicates an oscillatory motion, the accompanying real part determines the damping of that vibration. From 5 to 50 ms^{-1} an oscillating weave

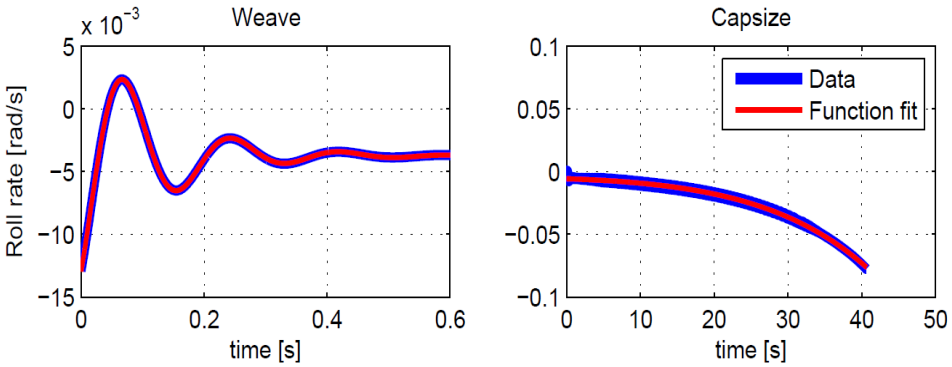

Figure 6. Response of the motorcycle roll rate at 10ms^{-1} left and 50 ms^{-1} right, with the identified weave and capsize response overlaid in the same graph.

motion could be identified from the impulse responses. A positive real eigenvalue is typical for the monotonous instable capsize mode. Qualitatively the presence of capsize and weave confirm the correct dynamics. The natural frequency of the weave is growing with increasing speed and

the damping decreases after initial increase. Although we found a qualitative match of the eigenvalues at the various driving speeds, quantitatively the results do not match with the rootloci in [25], whose parameters we borrowed. The weave natural frequency grows too large and the damping does not decrease to zero. Secondly we did not excite a wobble mode at wobble prone speeds even with alternative handle-bar impulse as model input. Avoiding extensive motorcycle parameter identification to populate e.g. Table 1 by borrowing Sharp's and Alstead's parameters has not been proven adequate by the determined root-loci. Further research is needed to see if this difference is caused by the tire model or other differences in the dynamics modeling.

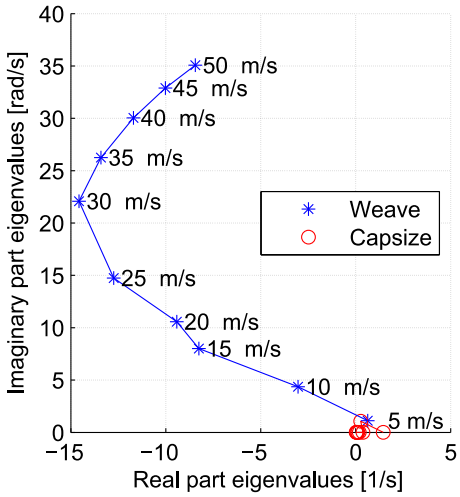

Figure 7. Root-loci of the simMechanics motorcycle model from 5 ms^{-1} to 50 ms^{-1}

3 MOTORCYCLE DRIVING SIMULATOR

The motorcycle model was integrated in an experimental motorcycle simulator with hexapod motion platform and head mounted display (Figure 2). The main components are described and evaluated below, and specifications are in Table 8 in the appendix. The rider interacts with the motorcycle's motion in various ways: How the rider controls the motorcycle using steer is described in 3.1, throttle and brakes are quite straightforward, The rider upper-body motion creates a roll torque. The influence of the roll torque on the attitude of the motorcycle model is subject of section 3.4. The platform provides vestibular cues according to the motion cueing algorithm of section 3.2, its dynamic performance is analysed in section 3.3. The HMD that provides visual motion cues is subject of section 3.5, next to these there is audio feedback to the rider.

3.1 Steering Control Loader

The handlebar is the most important interface for controlling a motorcycle. Therefore, correctness of its dynamic response is of great importance. With automotive and airplane simulators, the human input to the vehicle is generally a steering angle or position and feedback from the vehicle comes as force or torque created by a control loader. Motorcycle dynamics is governed by the front fork body and the mainframe having mass and inertia of the same order. For the motorcycle model the cross coupling between these two bodies form the essence of a proper dynamic model. While in a car model the dynamics of its steer rack can simply be substituted by imposed kinematics, imposing the handlebar angle on a motorcycle makes it lose its renowned self stabilizing property.

For the motorcycle simulator steering, the causality of the calculation is reversed and the rider's input to the vehicle model is now the measured steering torque, where the control loader controls the handlebar angle. The E2M eMoveRT controller offers this possibility by changing some firmware settings. As a build-in safety feature, the control software also comprises so

called ‘jam-override’ control. Its function is illustrated by the block scheme of Figure 8. There a force limiter ensures that no excessive forces can be generated which could eventually hurt or injure the user, even in position mode.

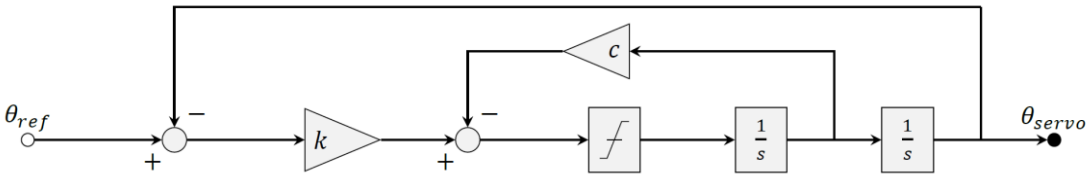

Figure 8. Bock scheme of jam-override function. A position tracking controller with a saturated controller force is always active in the position control loop. As a side effect of this implementation, a filter with finite bandwidth is included in the position control loop. The bandwidth of this filter can be configured in the GUI: 100 rads^{-1} and 500 rads^{-1} are used for identification.

The dynamic response of the control loader was experimentally evaluated and represented in the frequency domain, controlling the handlebar angle with hands off. Recorded signals included steering reference angle, steering angle, steering torque and motor current, collected at 1000 Hz. Two types of control inputs were applied. The first input was a chirp signal, ranging from 0.5 Hz to 40 Hz. A chirp signal is a sinusoidal signal with increasing frequency. The second control input was a Gaussian uniformly distributed random signal (white noise), filtered with a 40 Hz second order low pass filter.

Transfer functions were derived using the function tfestimate from the Signal Processing Toolbox in MATLAB®, with Welch’s averaging with a symmetric Hanning window. The magnitude squared coherence was derived using mscohere.

Figure 9 shows the steering assembly frequency response, with similar results for Chirp & Gaussian input types. The coherence was close to 1 up to 30 Hz for the Gaussian, and 20 Hz for the Chirp input. The adapted setting increased the effective bandwidth from ~20 Hz to ~30 Hz with a markedly improved phase lag also at lower frequencies. The phase lag in Figure 6 is equivalent to only ~0.02 s for the improved setting against 0.034 s for the original setting.

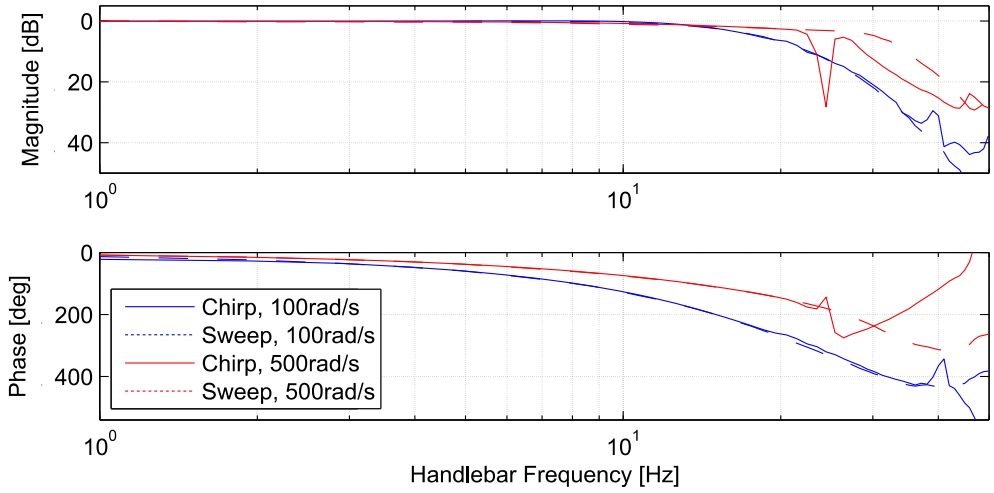

Figure 9. Steering system dynamics with gain (top) and phase (bottom) from reference angle to achieved angle. Blue signals represent the original setting 100 rads^{-1} and red signals the improved setting 500 rads^{-1}.

Initially the handlebar response of the simulator was not satisfactory. The above identification confirms that the handling of the motorbike benefits notably from increasing the parameters of the jam-override module from 100 rad/s to 500 rad/s. The dimensionless damping remained unchanged at 0.7.

3.2 Motion platform & cueing

Since a motion platform is limited by its workspace and dynamics, it is impossible to cue all motions exactly as experienced in a real vehicle. So-called motion cueing algorithms have been developed over the years e.g. [27] and are used in the motorbike simulator also. Acceleration, velocity and position signals coming from the vehicle dynamics model are scaled and filtered to keep the motion platform within its bounds. We employed a classical washout filter design illustrated in Figure 10 that is available as part of eMoveRT software. Here, DWM stands for Direct Workspace Management, a washout method using real-time optimization with a tunable penalization function to best use the platform range with minimal false cues [28]. As the motorcycle pitch and roll angle are physically bounded, these angles are applied using scaling factors with marginal low pass filtering to attenuate vibrations. Specific attention has been given to roll angle cueing. When riding a steady state corner on a 2-wheeler, the vector combination of lateral acceleration a_y and gravity g pushes the rider right into the saddle. Unfortunately, a constant lateral acceleration a_y cannot be cued by a motion platform. If we would apply the full unscaled roll, gravity would induce large and unrealistic roll moments on the rider body. Based upon trial evaluations we scaled the platform roll to 25% of the motorcycle roll. This is approach is similar to Shahar et al. [29] where participants favored 'roll in the turn' cueing.

Yaw rotation, and X, Y, Z translation are unbounded in reality, and highly constrained by the workspace of the hexapod. This is resolved using high pass filters providing so called 'onset cueing'.

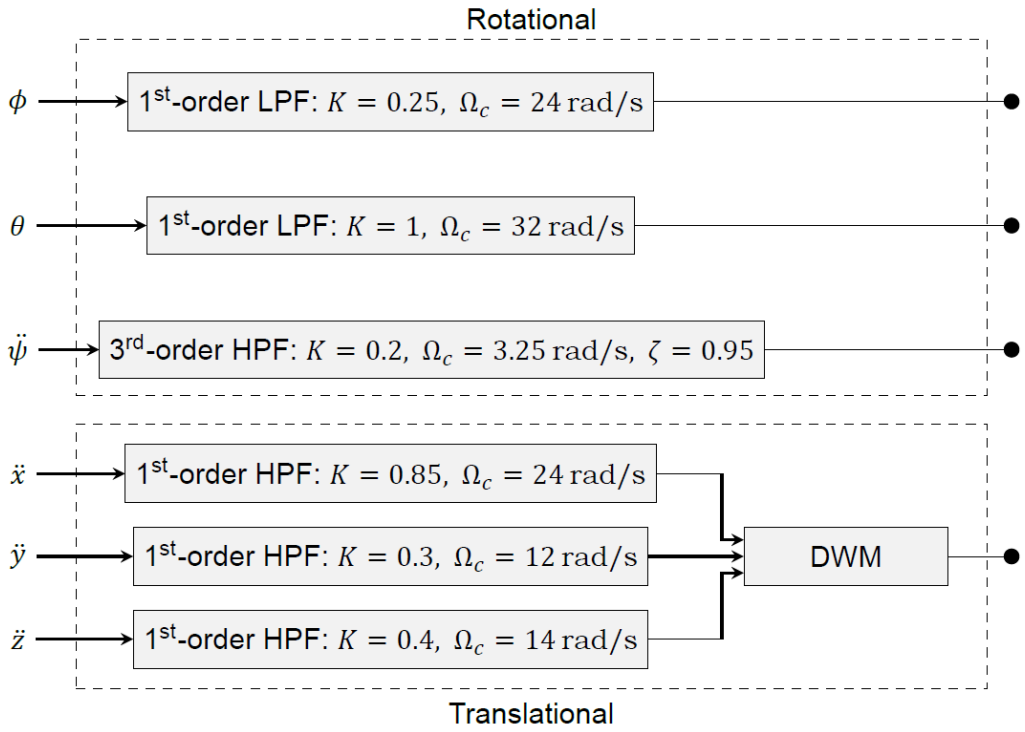

Figure 10. Motion cueing: Note that roll (φ) and pitch (θ) are position referenced and not acceleration referenced like the other signals. HPF is short for high-pass filter and DWM is short for Direct Workspace Management. Roll (φ) is scaled (25%) and low pass filtered (1st order 24 rad/s), pitch (θ) is not scaled (100%) and low pass filtered (1st order 32 rad/s), yaw (ψ) is scaled (20%) and high pass filtered (2nd) order, damping=0.95), X,Y,Z accelerations are scaled (85%, 30%, 40%) and high pass filtered (24, 12, 14 rad/s).

3.3 Motion platform bandwidth

The dynamic response of the motion platform has been evaluated using a similar approach as for the steering control loader. Instead of using a chirp or noise function as used for steering, the platform was excited at specific frequencies from 1 to 20 Hz in steps of 1 Hz with a pure sine function with an amplitude of 1 m/s^2 for translations and 0.7 rad/s^2 for rotations. This sine function determines the acceleration reference for all six degrees of motion individually (surge, sway, heave, roll, pitch, yaw). Again, the function tfestimate was used to obtain the frequency response characteristics.

Figure 11 shows the bode plot for the motion platform. It can be seen that until 10 Hz, the magnitude remains under 2.5 dB and with a phase lag below 10 deg. Around 11 to 12 Hz, a first resonance peak can be observed for the surge and sway, and to a lesser extend for pitch. At 18 Hz, the first resonance peak for heave can be seen. We may conclude that the motion platform is capable to reproduce the weave eigenmode at its natural frequency. A potential wobble mode will occur at a frequency beyond the bandwidth of the platform: the wobble shall be emulated with the handlebar control loader mainly.

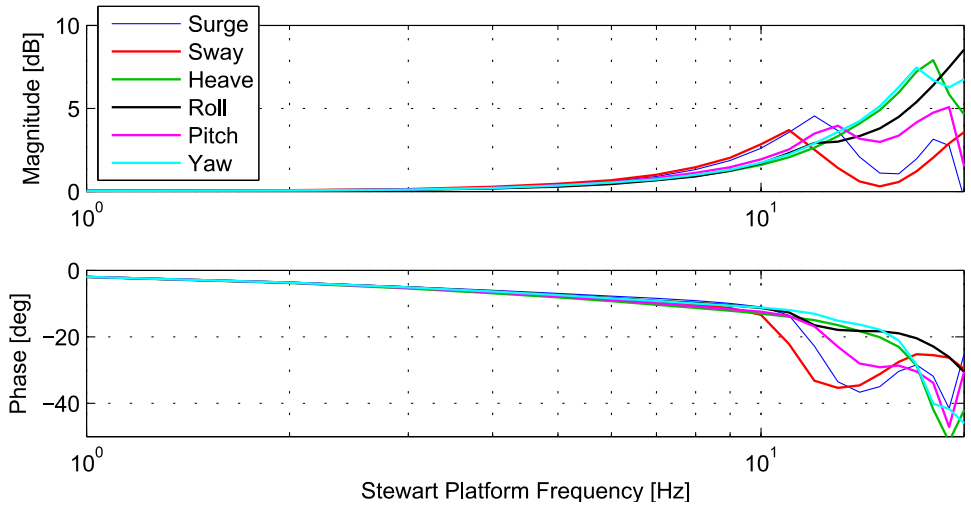

Figure 11. Bode plot for all 6-DoF of the motion platform. Translational and rotational motion are shown in solid and dashed lines respectively.

3.4 Upper Body Tracking

For the rider upper body tracking, two Intel RealSense SR300's [30] are mounted on the top platform see b in Figure 2. These cameras use coded light, also known as structured light to estimate 3d features at a distance from 0.2 – 1.5 m. Each camera features a full 1080p color camera at 30 frames per second to reconstruct hand gestures, shapes or facial features. Using data from both cameras, the rider upper body position is estimated. For the current experiments, only the lateral displacement of the rider body has been used, practically reducing the model order to 14-DoF (13 for the motorcycle and 1 for the rider). The lateral body motion generates a roll moment in the motorcycle model. In trials it was confirmed that most participants could thus manoeuvre with hands free at speeds above 50 km/h.

The upper-body position has been modeled as a separate upper rider body in SimMechanics™ which is connected to the main frame that includes the lower rider body. The connection is made with a prismatic joint that allows lateral movement. For this lateral movement a position controller can be written in Simulink, or a joint motion actuator can be exploited. A position controller that constantly calculates the internal force to reach and maintain the lateral upper body offset is true the physics. However, the measurement noise from the real-sense camera system introduces sensible lateral vibration into the motorcycle model. Eventually the kinematic joint actuator is preferred for implementation in the simulator.

3.5 Visual System

An Oculus Rift HMD provides the rider with visual cues, which are continuously adapted to the head motion. This is achieved using two different systems to track the head motion. The first system is called the constellation sensor, an infrared sensor placed in front of the rider (see a in Figure 2). The Rift includes a number of infrared LEDs, which are tracked by the constellation sensor. The second system is located inside the Rift self, featuring a magnetometer, a gyroscope and an accelerometer. At 1000 Hz, combining the information from the constellation sensor and the systems inside the HMD, the Oculus software is able to give an accurate estimation of the 6-DoF motion of the Oculus Rift in the real world. By calibrating the Oculus Rift if the motion platform is engaged but in resting state, the head position of the user can be accurately estimated. All translations and rotations from the motion platform are consequently compensated for, such that the visuals sent to the Oculus Rift correspond to where the user's head is in the virtual world.

To take a constant roll angle of 32° as an example, the motion platform cues 7° of roll and the HMD's horizon cues the complete 32° as illustrated in Figure 12. Note that the HMD visualizes the horizon with respect to the ego motorcycle at 32° to represent the motorcycle attitude in the virtual world. If an outside spectator could look at the HMD image he would see Figure 12b being rotated 7° clockwise. To the outsider the displayed horizon would be at 32° – 7° = 25° with respect to the earth inertial reference.

In case the roll angle would be cued 1:1 at 32° and the rider would sit upright along the motion platform's local z-axis, the same visuals as Figure 12b would still be presented with a horizon at 32°.To the outsider however the horizon would now be level. In short: the visual roll cueing is made independent of the physical roll cued by the platform. To that end the Oculus firmware and the rendering software discriminate between platform induced roll and head rotations.

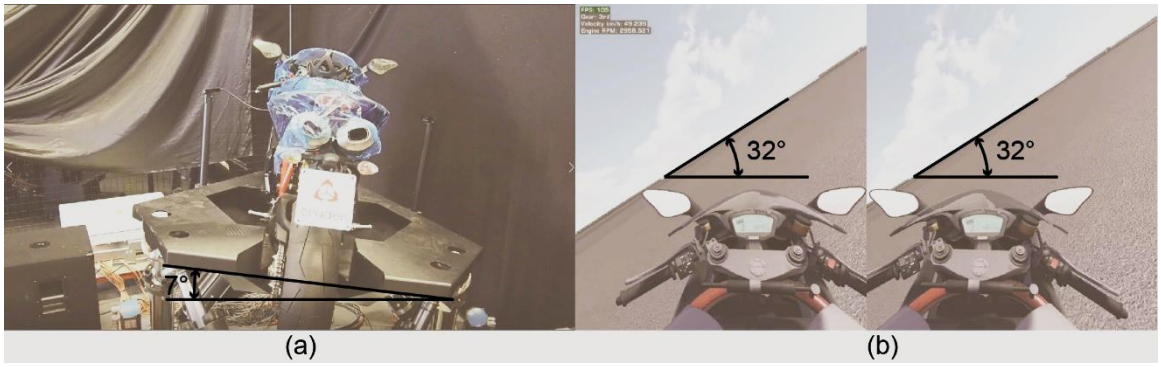

Figure 12. Roll cueing with the motion platform and the Oculus Rift. The Oculus Rift cues the complete roll angle (b), whereas the motion platform only cues 22% (a).

4 HUMAN IN THE LOOP EVALUATION

4.1 Participants

Participants with a valid motorcycle license were recruited via the social network of the first author (friends, colleagues). 16 participants were recruited, 15 successfully completed the speed perception experiment and 14 successfully completed the track following experiment. The average age of the participants was 29, with a standard deviation of 11 years. Most participants were students at the Delft University of Technology. Table 3 shows the distribution of years of ownership of a motorcycle license and the amount of kilometers ridden each year.

Before the experiments, participants had to complete an intake questionnaire addressing demographics, travel and riding behavior and previous experience with simulators. Participants were instructed on the operation of the motorcycle simulator, the safety procedures and the experiments, after which an informed consent form was signed. A simulator practice session was per-

formed (10 min) where participants were encouraged to ride both fast and slow and experience the dynamics of the motorcycle simulator. Participants were also asked to crash the motorcycle on purpose to experience such an event. Following the practice session, participants performed the speed perception (20 min) and trajectory tracking (60 min) experiments. The order of the two experiments was not randomized to gradually develop and harmonize the level of simulator experience within the two experiments. In all experiments, data was logged at 100 Hz.

Table 3 Distribution of license ownership and kilometers per year of the participants.

License ownership				
0-1 years	1-2 years	2-5 years	5-10 years	more than 10 years
1	2	2	7	4
km's ridden per year				
0-1000	1000-2000	2000-6000	6000-15000	more than 15000
5	5	3	3	0

4.2 Speed perception experiment

The speed perception test was conducted on a 9 kilometer long highway with 10 lanes of 3 m width. A graphical impression of the scenery is given in Figure 13. Three instructed speeds were tested in a randomized order with 3 repetitions (Table 4). After each tested speed, a break was held to complete a questionnaire. All speed perception tests were performed with platform motion and upper-body tracking.

When the participant thought he or she was riding the correct speed, he had to disengage the clutch and give a verbal stop sign, after which the experimenter stopped the simulation. The actual speed at clutch disengagement was extracted from the data, and for each instructed velocity, the 3 achieved velocities were averaged per participant.

Figure 13 Highway section used to perform speed perception experiments

Table 4 Experimental condition identifiers for the speed perception experiments (all with platform motion and upper-body tracking).

Experiment	Instructed Velocity	Identifier
Speed Perception	50 km/h	SP50-1
		SP50-2
		SP50-3
	80 km/h	SP80-1
		SP80-2
		SP80-3
	120 km/h	SP120-1
		SP120-2
		SP120-3

4.3 Speed perception results

Figure 14 and Table 5 show the main results, indicating a substantial scatter where speed is underestimated on average. For the reference velocity of 120 km/h one participant was constantly riding the maximum velocity of the motorcycle (200 km/h).

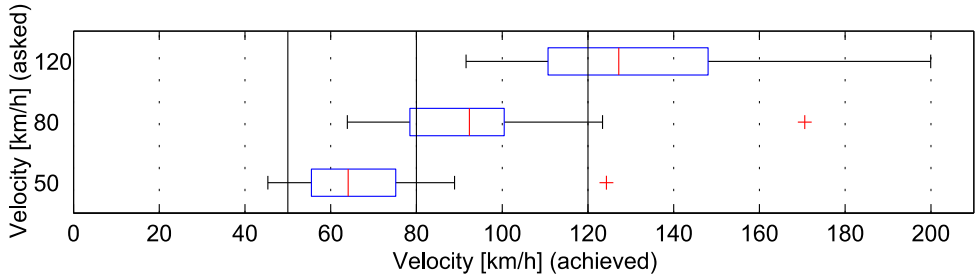

Figure 14. Speed driven for instructed speeds of 50, 80 and 120 km/h (vertical solid black lines). The red line in each box is the dataset median, the blue box the 25-75th % range, the whiskers extend to the most extreme data points not considered outliers, while red pluses are outliers.

Table 5 Speed driven with percentage differences towards the instructed speed.

Instructed	**Median**	diff.	**Mean**	diff.	min	max	**SD**
50 km/h	64.06 km/h	+28%	67.96 km/h	+36%	45.35 km/h	124.3 km/h	19.23 km/h
80 km/h	92.36 km/h	+15%	95.07 km/h	+19%	63.88 km/h	170.6 km/h	25.66 km/h
120 km/h	127.2 km/h	+6.0%	134.1 km/h	+12%	91.58 km/h	199.9 km/h	29.28 km/h

The underestimation of speed was expected from the literature [23][24] and results in Table 5 are in line with research by Recarte and Nunes on car driving [24], albeit that Table 5 shows somewhat larger standard deviations and more extreme outliers. It can be concluded that the participants were just as bad at estimating their velocity on a motorcycle simulator without speedometer as people driving in a car without a speedometer. This suggests that the combined visual, mechanical, and acoustic cues provide an adequate speed experience. However, multiple participants remarked that the contribution of wind noise was limited compared to riding on a real motorcycle. Interestingly, all participants were very curious on how they performed and were mostly unable to tell whether they were close to the demanded speed. This just underlines how difficult it is to estimate speed without a speedometer.

4.4 Path following experiment

The test participants were asked to follow a 2 m wide lane between cones on each side, consisting of straights and curves. The trajectory was approximately 1.3 km long and consisted of two 180° corners with 100 m radius followed by two 180° corners with 60 m radius. The straights between the corners were all 60 m long so that if participants failed to negotiate a corner, the straight was sufficiently long to return to the track. The designed layout of the track is illustrated in Figure 15 at the left, a birds-eye view on the start of the track is given at the right. Participants were asked to ride 50 km/h, resulting in non-critical accelerations (~1.9 m/s^2 and ~3.2 m/s^2 lateral accelerations for the 100 and 60 m radius curves respectively).

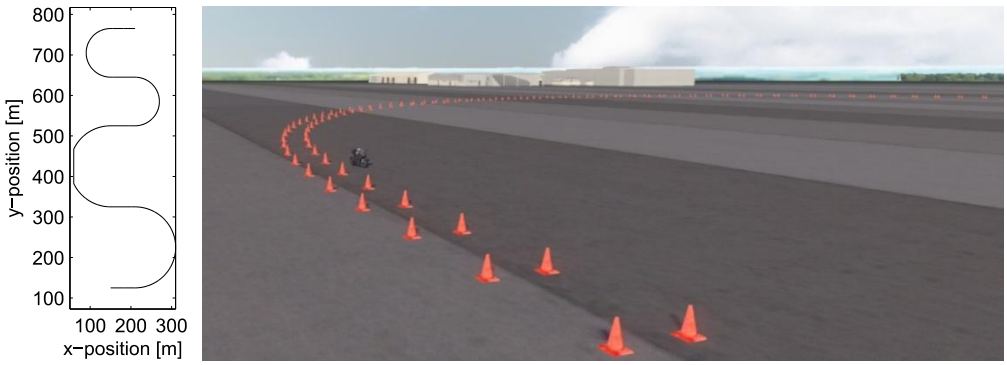

Figure 15 Path of semi-circular sections constituted by cones for the path following experiment.

Effects of motion cueing were evaluated for a) platform motion and b) upper body tracking, at two levels (on/off). A statistical 2x2 *within subject* experiment was performed, randomizing the order of the 4 conditions (see Table 6).

Table 6 Experimental conditions for the path following experiments.

Experiment	Motion	Body Tracking	Identifier
Trajectory Tracking	Motion	Tracking	M1T1
		No Tracking	M1T0
	No Motion	Tracking	M0T1
		No Tracking	M0T0

The statistical *within subject* approach was selected as simulator experiments tend to result in profound between participant differences, in particular for motion sickness. Hence, a *between participant* design would require an impractically large population. To minimize carry-over effects which include fatigue, interaction between conditions and learning effects, several measures have been taken, the 4 conditions in Table 6 were tested in a randomized order, and breaks were held between conditions to let the participant get some rest and have the participant fill in questionnaires about their experience. To avoid bias participants were not informed of the specific motion condition. Participants were not explicitly told to actively move their upper body and were just asked to ride normally. To have no body tracking during the simulation, the signals from the body lean sensors were simply ignored, resulting in the simulation of a stiff rider on the motorcycle.

After all experiments had been completed, the participants were asked to fill in one final form with general questions about the experiment and the motorcycle simulator. If there was some time left, the participants were invited to ride a few laps on one of the racing circuits available at the simulator, like Jerez or Zandvoort.

Statistics

In preliminary statistical analyses, few significant effects were found for body tracking, and visual inspection gave the impression that participants were hardly using their upper bodies to control the motorcycle simulator. Platform motion did have relevant and significant effects. Hence, we present main effects of platform motion lumping data with and without body tracking. Effects of upper body tracking were evaluated separately with and without platform motion, and only significant effects will be mentioned in the text.

Data for path following performance is usually not normally distributed as the lane deviation metrics are sensitive to single lane departures. For that reason, the Wilcoxon signed rank test was used, where the significance threshold was selected to be $\alpha = 0.05$.

4.5 Path following results

One participant was unable to complete the conditions without motion as these made him feel too uncomfortable, resulting in a full dataset with 14 participants. These 14 participants report a wide range of results for the Simulator Sickness Questionnaire (Figure 16), where for the 4 conditions 40-60% of the participants report no or minor sickness (SSQ<10).

Figure 17 shows lane deviations, and Figure 18 and Figure 19 show subjective evaluation of presence and workload. Table 7 shows detailed values, also including steer torque, and velocity.

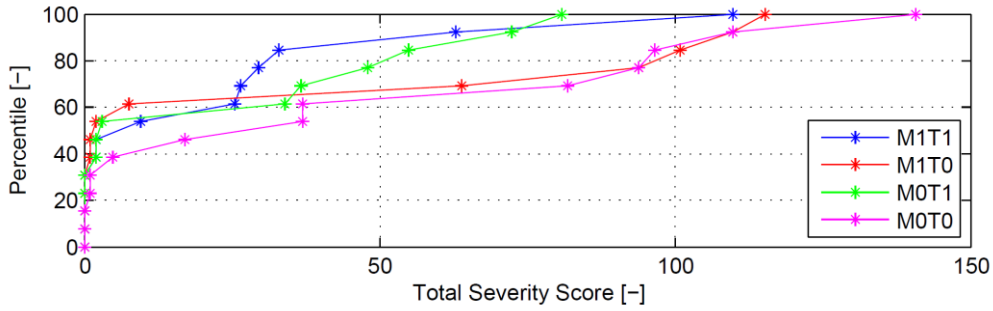

Figure 16. Simulator Sickness Questionnaire (SSQ) [31], cumulative distribution for the four simulator settings, maximum possible severity score = 160.72.

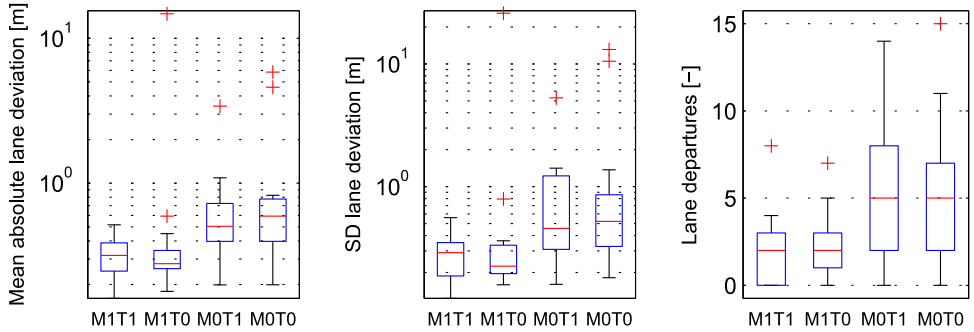

Figure 17. Boxplots for the mean absolute lane deviation, Standard Deviation (SD) and number of lane departures per 4 curves. Note that the y-axis is logarithmic to better show the distribution of data points for the mean absolute lane deviation and the standard deviation of lane deviation.

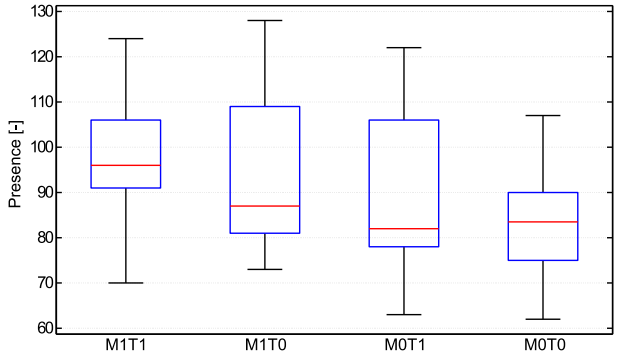

Figure 18. Overall presence in the range 0–140 [32].

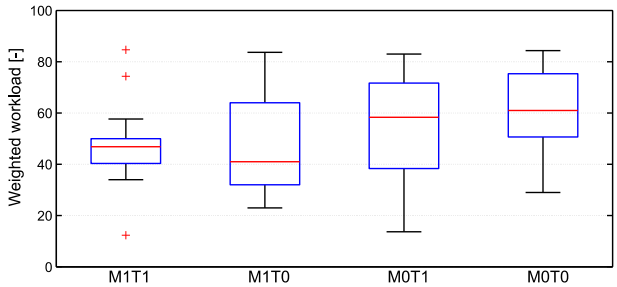

Figure 19. Overall workload according to the Task Load Index (TLX) range 0–100 [33].

Table 7 Wilcoxon signed rank test results for the main metrics and sub metrics. The motion and no-motion columns show the data medians for each lumped category respectively. Statistically significant p-values are boldfaced.

	Motion	**No-motion**			
Metric	*Med.*	*Med.*	p	Z	r
NASA-TLX					
Overall workload	43.75	56.75	**0.0131**	2.48	0.66
Mental Demand -	11.00	12.75	0.0684	1.82	0.49
Physical Demand -	8.00	11.75	**0.0302**	2.17	0.58
Temporal Demand -	7.50	7.75	0.5911	0.54	0.14
Performance -	8.50	10.0	0.1871	1.32	0.35
Effort -	10.75	14.00	**0.0169**	2.39	0.64
Frustration -	7.50	9.00	**0.0125**	2.50	0.67
Presence Questionnaire					
Overall presence	95.75	85.75	**0.0097**	2.59	0.69
Control factors -	48.25	44.00	0.2345	1.19	0.32
Sensory factors -	32.25	24.00	0.4797	0.72	0.19
Realism factors -	17.75	18.50	0.2345	1.19	0.32
Distraction factors -	9.75	9.00	0.2846	1.07	0.29
Simulator Sickness Questionnaire					
Total severity	3.37	13.97	0.2210	1.22	0.33
Nausea -	14.31	23.85	0.0685	1.82	0.49
Oculomotor discomfort -	7.58	13.27	0.1962	1.29	0.35
Disorientation -	24.36	13.92	1.0000	0.00	0.00
Lane keeping					
Lane departures	1.50	4.50	**0.0037**	2.91	0.78
Mean absolute lane center deviation	0.30 m	0.59 m	**0.0132**	2.48	0.66
Standard deviation lane center deviation	0.26 m	0.52 m	**0.0110**	2.54	0.68
Steer torque [Nm]					
Mean absolute steer torque	4.66	4.48	0.5098	0.66	0.18
Standard deviation steer torque	3.89	3.94	0.5098	0.66	0.18
Velocity [km/h]					
Average velocity	50.89	51.28	0.8261	0.22	0.06

Both performance and subjective evaluation show beneficial effects of platform motion. All metrics of lane deviation, and the overall values of workload and presence, show relevant and significant effects. Interestingly though, about one-third of the participants were unable to tell whether they were riding with or without motion after the experiments were completed. At the same time, one of the participants was unable to complete the experiments without motion. This indicates substantial personal preferences with respect to motion, as also observed by Ried and Nahon [18].

For upper body tracking only one significant effect was found: with body tracking a lower sickness was reported (median SSQ=2.5 with body tracking compared to SSQ=27 without body tracking) comparing conditions without platform motion. However, due to extreme differences between participants this difference was only just significant (p=.04, without correction for multiple testing). Furthermore, this beneficial effect of upper body tracking was not found with platform motion. It was observed during the experiments that some riders were not using their upper body as much as expected, which could be explained by trajectory driven. Riding 50 km/h, cornering did not require the participants to seek the limits of the motorcycle's handling capabilities, and thus did not require riders to use their upper body to steer the motorcycle, which could explain the inconclusive benefits of upper body tracking. Real-life experiments with a wider range of conditions, measuring actual upper body motions are recommended to validate and enhance the implemented body tracking, in conjunction with other simulator properties.

5 CONCLUSIONS

The multibody motorcycle model performs qualitatively well as the virtual motorbike in a driving simulator. Countersteer behaviour was present and the weave and capsize mode could be identified. An unstable wobble mode could not be identified in a driven speed range of 5-200 km/h. Potentially it could have been suppressed by the steer damping in our model or differences in tire modeling and frame flexibility.

The bandwidth of the motion platform 8-10Hz turned out to be sufficient to regenerate the weave and capsize mode on the platform, besides the in-plane dynamic behavior of the motorcycle. The wobble mode, should it occur, needs to be regenerated by the handlebar control loader since its natural frequency lies beyond the bandwidth of the motion platform. In particular the handlebar frequency response functions confirm that the handlebar response noticeably benefits from configuring its jam-override bandwidth to 500 $rads^{-1}$.

The speed perception experiments show that riders on a motorcycle simulator are just as bad in estimating their speed as car drivers, consequently underestimating their speed. Three hypotheses for the speed perception are confirmed: quantitatively the median is a little better and the mean estimated speed is a little worse than the percentages stated in the hypothesis. Reproducing more realistic wind was proposed as a helpful cue by many participants.

From the path tracking experiments, the main and statistically significant conclusions are that the workload and presence questionnaires confirm that platform motion improves the presence and reduces the workload. Three objective metrics on the path tracking performance: Lane departures, mean absolute deviation and standard deviation all show significant difference to support the need for motion on a motorcycle simulator. In conclusion: a motorcycle simulator needs motion for the rider to perform best.

The upper body tracking by means of infrared proximity sensors has not shown any significant difference in performance of the participants. We remark that the participants were not explicitly trained on the simulator in the use of the sensors, nor were they asked to actively exploit their gesture during the manoeuvres.

Hence we conclude that the Cruden motorcycle simulator as presented and evaluated in this paper is ready to be used in motorcycle research

5.1 Outlook

The quantitative mismatch between the root-loci of the simMechanics multi-body model and the results directly from Sharp and Alstead [25] require investigation in the cause of the mismatch. Meanwhile we should also get a wobble mode excited in the motorbike model.

In general, the conclusion that the speed perception on the motorcycle simulator is realistic since it was just as poor as in a car is can be argued. We shall look into the generation of wind on the simulator, and need to retune the wind noise audio.

REFERENCES

[1] Hans B. Pacejka, *Tyre and Vehicle Dynamics*, Butterworth and Heinemann, Oxford, 2002.

[2] Robin S. Sharp, "The stability and control of motorcycles", Proceedings of the IMechE, Part C, *Journal of Mechanical Engineering Science*, **13**(5) pp. 316-329, 1971.

[3] E. Bertolazzi, F. Biral, M. Da Lio and V. Cossalter, "The influence of rider's upper body motions on motorcycle minimum time maneuvering", in C. L. Bottasso, P. Masarati and L. Trainelli (eds), *Proceedings Multibody Dynamics 2007*, ECCOMAS Thematic Conference, Milano, Italy, 25-28 June 2007, Politecnico di Milano, Milano, 2007, 15 pp.

[4] NHTSA. "Motorcycles traffic safety fact sheet" (dot-hs810-990). https://crashstats.nhtsa.dot.gov/Api/Public/ViewPublication/810990, 2007. accessed: 14-11-2017

[5] Shingo Chiyoda, Kenichi Yoshimoto, Daisuke Kawasaki, Yoshifumi Murakami, and Takayuki Sugimoto. "Development of a motorcycle simulator using parallel manipulator and head mounted display". *Proceedings of the International Conference on Motion and Vibration Control* 6.1, pages 599–602. The Japan Society of Mechanical Engineers, 2002.

[6] Vittore Cossalter, Roberto Lot, Matteo Massaro, and Roberto Sartori. "Development and validation of an advanced motorcycle riding simulator". *Proceedings of the Institution of Mechanical Engineers, Part D: Journal of Automobile Engineering*, **225**(6):705–720, 2011.

[7] D. Ferrazzin, FBACA Salsedo, F Barbagli, CA Avizzano, G Di Pietro, A Brogni, M Vignoni, M Bergamasco, L Arnone, M Marcacci, et al. "The moris motorcycle simulator: an overview". Technical report, SAE Technical Paper, 2001.

[8] Lamri Nehaoua, Salim Hima, Hichem Arioui, Nicolas Seguy, and Stéphane Espié. "Design and modeling of a new motorcycle riding simulator". In American Control Conference, 2007. ACC'07, pp. 176–181. IEEE, 2007.

[9] Alex W. Stedmon, Benjamin Hasseldine, David Rice, Mark Young, Steve Markham, Michael Hancox, Edward Brickell, and Joanna Noble. "'motorcyclesim': an evaluation of rider interaction with an innovative motorcycle simulator". *The Computer Journal*, **54**(7):1010–1025, 2009.

[10] Francis J.W. Whipple. "The stability of the motion of a bicycle". *Quarterly Journal of Pure and Applied Mathematics*, **30**(120):312–321, 1899.

[11] J. P. Meijaard, Jim M. Papadopoulos, Andy Ruina, A. L. Schwab, 2007 ``Linearized dynamics equations for the balance and steer of a bicycle: a benchmark and review," *Proceedings of the Royal Society A* **463**:1955-1982.

[12] Cornelis Koenen. *The dynamic behaviour of a motorcycle when running straight ahead and when cornering. PhD thesis*, Delft University of Technology, 1983.

[13] Vittore Cossalter and Roberto Lot. "A motorcycle multi-body model for real time simulations based on the natural coordinates approach". *Vehicle system dynamics*, **37**(6):423–447, 2002.

[14] David J.N. Limebeer and Robin S. Sharp. "Bicycles, motorcycles, and models". *IEEE control systems*, **26**(5):34–61, 2006.

[15] Vittore Cossalter, Roberto Lot, and Stefano Rota. "Objective and subjective evaluation of an advanced motorcycle riding simulator". *European transport research review*, **2**(4):223–233, 2010.

[16] Keith Code. *A twist of the wrist Volume II*. California Superbike School, Inc., 1993

[17] Jacob A Houck, Robert J Telban, and Frank M Cardullo. *Motion cueing algorithm development: Human-centered linear and nonlinear approaches.* 2005.

[18] Lloyd D Reid and Meyer A Nahon. "Response of airline pilots to variations in flight simulator motion algorithms". *Journal of Aircraft*, **25**(7):639–646, 1988.

[19] Andras Kemeny and Francesco Panerai. "Evaluating perception in driving simulation experiments". *Trends in cognitive sciences*, 7(1):31–37, 2003.

[20] Gilles Reymond, Andras Kemeny, Jacques Droulez, and Alain Berthoz. Role of lateral acceleration in curve driving: “Driver model and experiments on a real vehicle and a driving simulator”. *Human factors*, **43**(3):483–495, 2001.

[21] Walter W. Wierwille, John G. Casali, and Brian S Repa. “Driver steering reaction time to abrupt-onset crosswinds, as measured in a moving-base driving simulator”. *Human Factors*, **25**(1):103–116, 1983.

[22] Hirohide Imaizumi, Takehiko Fujioka, and Manabu Omae. “Rider model by use of multibody dynamics analysis”. *JSAE review*, **17**(1):75–77, 1996.

[23] Sebastian Will. *Development of a presence model for driving simulators based on speed perception in a motorcycle riding simulator*. Inaugural-dissertation, Fakultät für Humanwissenschaften der Julius-Maximilians-Universität Würzburg, 2017.

[24] Miguel A. Recarte and Luis M. Nunes. “Perception of speed in an automobile: Estimation and production”. *Journal of experimental psychology: applied*, **2**(4):291, 1996.

[25] R.S. Sharp and C.J. Alstead. “The influence of structural flexibilities on the straight-running stability of motorcycles”. *Vehicle system dynamics*, **9**(6):327–357, 1980.

[26] Edwin J.H. de Vries and Hans B. Pacejka. “Motorcycle tyre measurements and models”. *Vehicle system dynamics*, **29**(S1):280–298, 1998.

[27] Meyer A. Nahon and Lloyd D. Reid. “Simulator motion-drive algorithms - A designer's perspective”, *Journal of Guidance, Control, and Dynamics*, **13**(2): 356–362, 1990

[28] Veltena M.C. Movement Simulator, US Patent # 8,996,179, March 31, 2015

[29] Amit Shahar, Virginie Dagonneau, Séphane Caro, Isabelle Israël, and Régis Lobjois. “Towards identifying the roll motion parameters of a motorcycle simulator”. *Applied ergonomics*, **45**(3):734–740, 2014.

[30] Intel RealSense Technology. Intel realsense camera sr300. https://software.intel.com/en-us/realsense/sr300, 2018. Accessed June 12, 2018.

[31] Robert S. Kennedy, Norman E. Lane, Kevin S. Berbaum, and Michael G. Lilienthal. “Simulator sickness questionnaire: An enhanced method for quantifying simulator sickness”. *The international journal of aviation psychology*, **3**(3):203–220, 1993.

[32] Bob G Witmer and Michael J Singer. “Measuring presence in virtual environments: A presence questionnaire”. *Presence*, **7**(3):225–240, 1998.

[33] Sandra G Hart and Lowell E Staveland. “Development of nasa-tlx (task load index): Results of empirical and theoretical research”. *Advances in psychology* **52**, pp. 139–183. Elsevier, 1988.

APPENDIX

The Panthera software developed by Cruden integrates the vehicle dynamics, vision, audio and motion platform control. Panthera runs on all PC's except for the
E2M RealTime PC.

Table 8 Motorcycle simulator specifications.

Motion Platform	
Stewart platform	E2M eM6-300-1500 [37]
Control loader	E2M eF-DD-50 [36]
Real-time PC	Linux RT/Xenomai + eMoveRT controller
Communication protocol	UDP + EtherCAT
Motorcycle Mock-Up	
Model	Ducati 848 Evo
Steering torque sensor	Loadcell Transducer Techniques
Body position sensor	Intel RealSense SR300 Dev kit (2x) [38]
Throttle position sensor	Potentiometer 75mm PM2S-75-5K
Gear selection sensor	Interlock Switch shifter unit
Clutch sensor	Brake sensor, 250 bar
Front brake sensor	Brake sensor, 250 bar
Rear brake sensor	Brake sensor, 250 bar
Kill cord for interlock	Demon Tweeks: Bike-It Universal Kill Switch With Tether
Computer hardware	
Computers	- Operator/Database PC - Telemetry PC - GPS tracker PC - Spectator PC - HMD PC
Graphics cards	NVIDIA GeForce GTX 1080
Processors	Intel i7-6700K (Master) Intel Xeon X3350 (Others)
Memory	16 GB at 1666MHz
Sound Card(s)	Creative Soundblaster Z PCIe
Communication	Ethernet
Video	
Head mounted display	Oculus Rift
Display	2,160 x 1,200 pixels, OLED
Refresh rate	90 Hz
Audio	
Mixer	Allen & Heat GR4 4ch mixer with ducking
Amplifiers	Yamaha P2500S Amp (3x)
Speakers	Yamaha SW115W Subwoofer
Speakers	Yamaha SM10V Floor monitor (4x)
Speakers	Yamaha MS101 III Active speaker for intercom talkback